

A large eddy simulation on the effect of buildings on urban flows

Ning Zhang[†]

Department of Atmospheric Science, Nanjing University, Nanjing, 210093, China

Weimei Jiang[‡]

*Department of Atmospheric Science, Nanjing University, Nanjing, 210093, China
Key Laboratory of Atmospheric Physics and Chemistry, Institute of Atmospheric Physics, Chinese Academy of Sciences, Beijing, 100029, China*

Shiguang Miao^{‡†}

Beijing Meteorology Bureau, Beijing, 100089 China

(Received January 12, 2005, Accepted November 16, 2005)

Abstract. The effect of buildings on flow in urban canopy is one of the most important problems in local/micro-scale meteorology. A large eddy simulation model is used to simulate the flow structure in an urban neighborhood and the bulk effect of the buildings on surrounding flows is analyzed. The results demonstrate that: (a) The inflow conditions affect the detailed flow characteristics much in the building group, including: the distortion or disappearance of the wake vortices, the change of funneling effect area and the change of location, size of the static-wind area. (b) The bulk effect of the buildings leads to a loss of wind speed in the low layer where height is less than four times of the average building height, and this loss effect changes little when the inflow direction changes. (c) In the bulk effect to environmental fields, the change of inflow direction affects the vertical distribution of turbulence greatly. The peak value of the turbulence energy appears at the height of the average building height. The attribution of fluctuations of different components to turbulence changes greatly at different height levels, in the low levels the horizontal speed fluctuation attribute mostly, while the vertical speed fluctuation does in high levels.

Keywords: large eddy simulation; urban canopy; buildings; air flow.

1. Introduction

The numerical simulation on urban meteorological environment began since 1960s (Myrup 1969). In the early numerical simulations the aerodynamics effect of urban canopies on boundary layer is

[†] PhD Student, E-mail: zhangning_odin@yahoo.com.cn

[‡] Professor, Corresponding Author, E-mail: wmjiang@jlonline.com

^{‡†} Research Associate, E-mail:sgmiao@ium.cn

taken in account as an increase of the magnitude of surface roughness, (Yu 1975, Gutman and Torrance 1975, Vukovich 1976, 1978, 1979 for example). It is an effective method in low-resolution simulations while in a high-resolution modeling, which is of a resolution of 1–10 km, the parameterization method is too simple to describe the fine physical processes related with the buildings effect. Sorbjan (1982) parameterizes the damp and fluctuation of buildings in an urban canopy in the equations of motion and turbulence energy, which are used in numerical modeling on forest canopies. This method proves to be successful and is used widely now. Uno (1989) develops a model with parameterization of the damp and fluctuation of buildings and the heterogeneity of the distribution intensity and height of buildings and simulates the night boundary layer above an ideal city.

Besides the research on the meso-scale urban effect, the local-scale and micro-scale urban meteorological environment study is among the research focuses. The numerical research on local/micro scale urban meteorological environment is important in two aspects in brief: (a) The detail information supplied by the small scale numerical results will be helpful to develop and improve the parameterization of urban area in meso-scale modeling; (b) a detail flow field is the basis to predict the atmosphere pollutant dispersion in urban canopies. Urban canopies are the most important areas where people are living and working, and where pollutants are released densely. It is helpful for improving the living quality and protecting the safe of the residence to investigate the meteorological environment.

In the previous works, most of the studies in this field are carried out with RANS (Reynolds Averaged Navier-Stocks) models (Paterson and Apelt 1986, 1989, 1990, Summers and Hanson, *et al.* 1986, Murakami and Mochida 1988, Hunter 1992, Baskaran and Kashef 1996, Sini 1996, Ashie 1999, Baik and Kim 1999, Kim and Baik 1999, Jiang and Miao, *et al.* 2003, Zhang, Jiang, *et al.* 2004, Kim and Baik 2004 for example), the $k-\varepsilon$ turbulence energy closure scheme is one of the most popular means, and LES (Large Eddy Simulation) models are being used as well in many fields (Murakami and Mochida 1988, He and Song 1997, Shah and Freziger 1997, Jiang and Miao 2004, Miao and Jiang 2004 for example). The RANS method has been well developed and employed widely, while there are many deficiencies in using (Zhang, Jiang, *et al.* 2004). Murakami, *et al.* (1990) compare RANS method and LES method with a wind tunnel experiment dataset to investigate their skill in modeling the flow characteristics around a building. It shows that LES works better especially in modeling the flow structures near wall and the turbulence field. Tutar and Oguz (2002) couple the LES method with a CFD software to model flows between two buildings and explain the buildings' effect on the channeling effect well. In this paper, a LES model is used to model the buildings' effect on flows in a building group in urban canopy. Tutar and Oguz (2004) also compared the performance of the RNG $k-\varepsilon$ model and the large eddy simulation approach, the LES techniques are promising to study the atmospheric boundary layer field compared with the RANS means.

2. Description the numerical model and cases

2.1. Description of the model

A LES model is established by Zhang (2004) to simulate the flows in urban neighborhoods. This model includes the equations of continuity, motion and thermal, the TKE sub-grid scheme is used, which is developed by Deardorff (1980).

The equations are:

$$\frac{\partial \bar{u}}{\partial x} + \frac{\partial \bar{v}}{\partial y} + \frac{\partial \bar{w}}{\partial z} = 0 \quad (1)$$

$$\frac{\partial \bar{u}_i}{\partial t} = -\frac{\partial \bar{P}^*}{\partial x_i} - \bar{u}_i \frac{\partial \bar{u}_i}{\partial x_j} - \frac{\partial \tau_{ij}}{\partial x_j} \quad (2)$$

$$\frac{\partial \bar{\theta}}{\partial t} = -\bar{u}_j \frac{\partial \bar{\theta}}{\partial x_j} - \frac{\partial \tau_{\theta j}}{\partial x_j} \quad (3)$$

Here, \bar{u}_i ($i=1,2,3$) are resolvable velocity components; $\bar{\theta}$ is resolvable potential temperature;

$$\tau_{ij} = -2K_m S_{ij} \quad (4)$$

$$S_{ij} = \left(\frac{\partial \bar{u}_i}{\partial x_j} + \frac{\partial \bar{u}_j}{\partial x_i} \right) \quad (5)$$

$$\tau_{\theta j} = -K_h \frac{\partial \bar{\theta}}{\partial x_j} \quad (6)$$

$$\bar{P}^* = \frac{\bar{P}}{\rho_0} + \frac{R_{kk}}{3} \quad (7)$$

$$K_m = C\lambda e^{1/2} \quad (8)$$

e refers for sub-grid turbulence energy:

$$\frac{\partial e}{\partial t} = -\bar{u}_j \frac{\partial e}{\partial x_j} - \overline{u'_i u'_i} \frac{\partial \bar{u}_i}{\partial x_j} + \frac{\overline{w'\theta'}}{\theta_0} g - 2K_m \frac{\partial^2 e}{\partial x_i^2} - \varepsilon \quad (9)$$

The dissipation of turbulence kinetic energy is calculated by:

$$\varepsilon = \frac{C_\varepsilon e^{3/2}}{\lambda} \quad (10)$$

C and C_ε are constants; $C = 10.0$, $C_\varepsilon = 0.19 + 0.74\lambda/\Delta$

Δ is a length scale and defined by:

$$\Delta = \left(\frac{3}{2}\Delta_x \frac{3}{2}\Delta_y \Delta_z \right)^{1/3} \quad (11)$$

$\lambda = \Delta$ for neutral and convective stratification and $\lambda = \min \left[\Delta, 0.76e^{1/2} \left(\frac{g}{\theta_0} \frac{\partial \theta}{\partial z} \right)^{-1/2} \right]$ for stable, (12)

$$K_h = (1 + 2\lambda/\Delta)K_m \quad (13)$$

These equations are solved in a Cartesian coordination and the effect of building is simulated explicitly. The wall function approach of Launder and Spalding (1974) is used to bridge the

viscosity-affected region between the wall and the fully turbulent region as in the works of Zhang, Jiang (2004).

2.2. Validation of the model

One of the physical simulation cases of CEDVAL* wind tunnel experiment (case number: A1-1) is modeled with the numerical model to test the validation of the numerical simulation. Wind tunnel experiment case A1-1 is to investigate the wind field around a bluff building; the height, width, and length of the building are 25 m, 30 m, and 20 m. The inlet flow condition of both physical experiment and numerical simulation is: $u = u_0 \left(\frac{Z}{Z_0} \right)^a$, $v = 0$ m/s, $w = 0$ m/s, $a = 0.20$, $u_0 = 6.0$ m/s, $z_0 = 100$ m. The numerical simulation domain is $500 \text{ m} \times 500 \text{ m} \times 300 \text{ m}$ with a resolution of 2 m. The initial and lateral conditions are same in both numerical experiment and physical experiment. The lateral

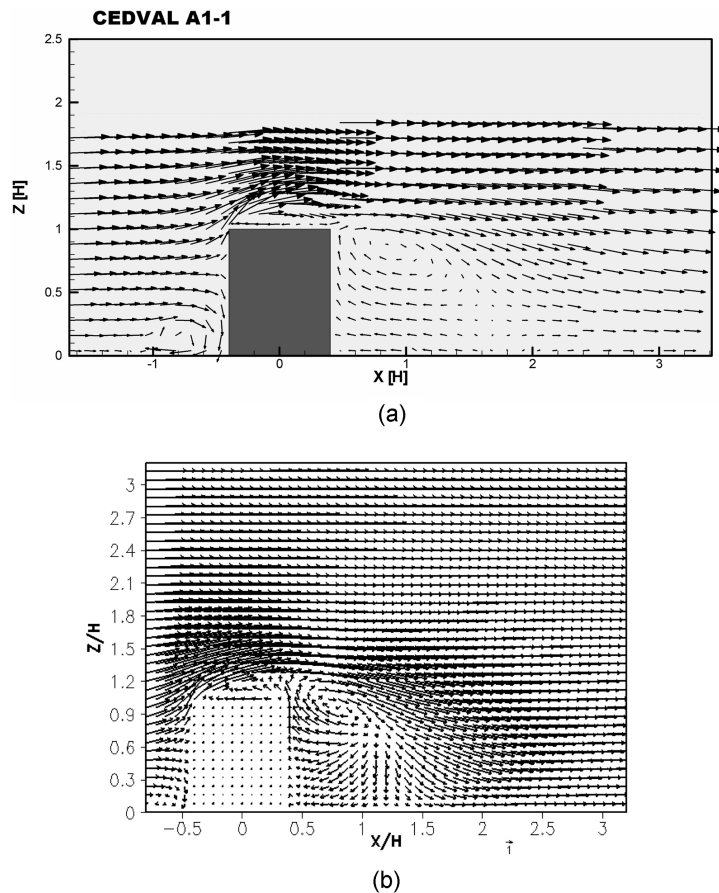


Fig. 1 The vertical cross-section of wind vector field: (a) CEDVAL result (b) LES result (20-min average)

*Refer to <http://www.mi.uni-hamburg.de>

condition is zero-gradient condition, and the bottom condition is no-skip solid condition. The whole simulation time is 30 minutes, and the results of the last 20 minutes are averaged to get the average field.

The results of the physical simulation and the numerical one are compared both in the whole flow field (as shown in Fig. 1) and in the velocity components profiles of u and w (in Fig. 2 and Fig. 3). The numerical results agree well with the physical ones on the whole (Detailed information refers to Zhang 2004 and Zhang and Jiang 2005).

The numerical simulation results of the large eddy simulation model agree well with the CEDVAL wind tunnel experiment results and can describe the reverse flows which above the building roof and beside the building in a good detail. The numerical simulated flow structures behind the building have some errors from the wind tunnel experiment, especially the w component as shown in Fig. 3(c). The reason causing these errors are mainly that the different of the cavity structure of numerical simulation and physical simulation. The cavity vortex structure in wind tunnel experiment is eclipse which upper part is compressed, the long axis of it is parallel with the surface, while in numerical simulation result, the shape of the cavity vortex is a regular eclipse, and there is a sharp

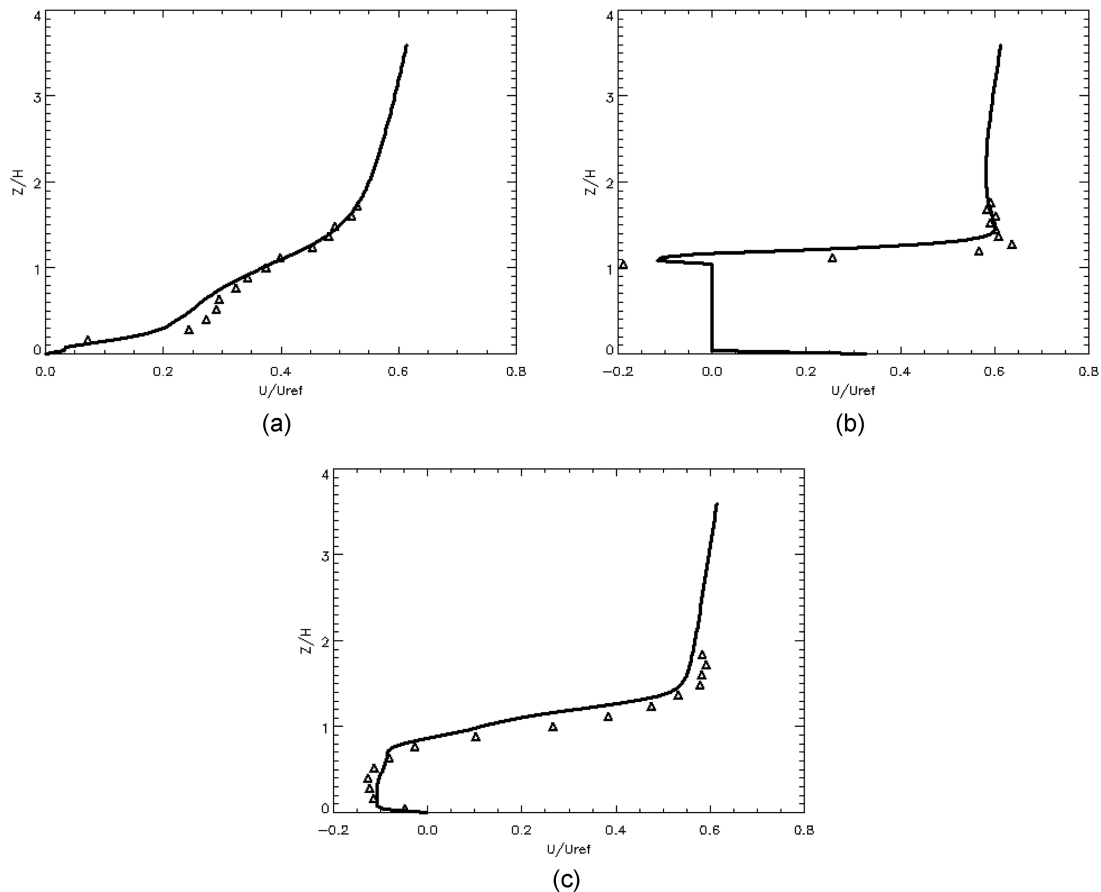


Fig. 2 The comparison of vertical profiles of u -component between CEDVAL and LES result (20-min average): (a) $X/H = -0.82$; $Y/H = 0$ (b) $X/H = -0.08$; $Y/H = 0$ (c) $X/H = 1.08$; $Y/H = 0$

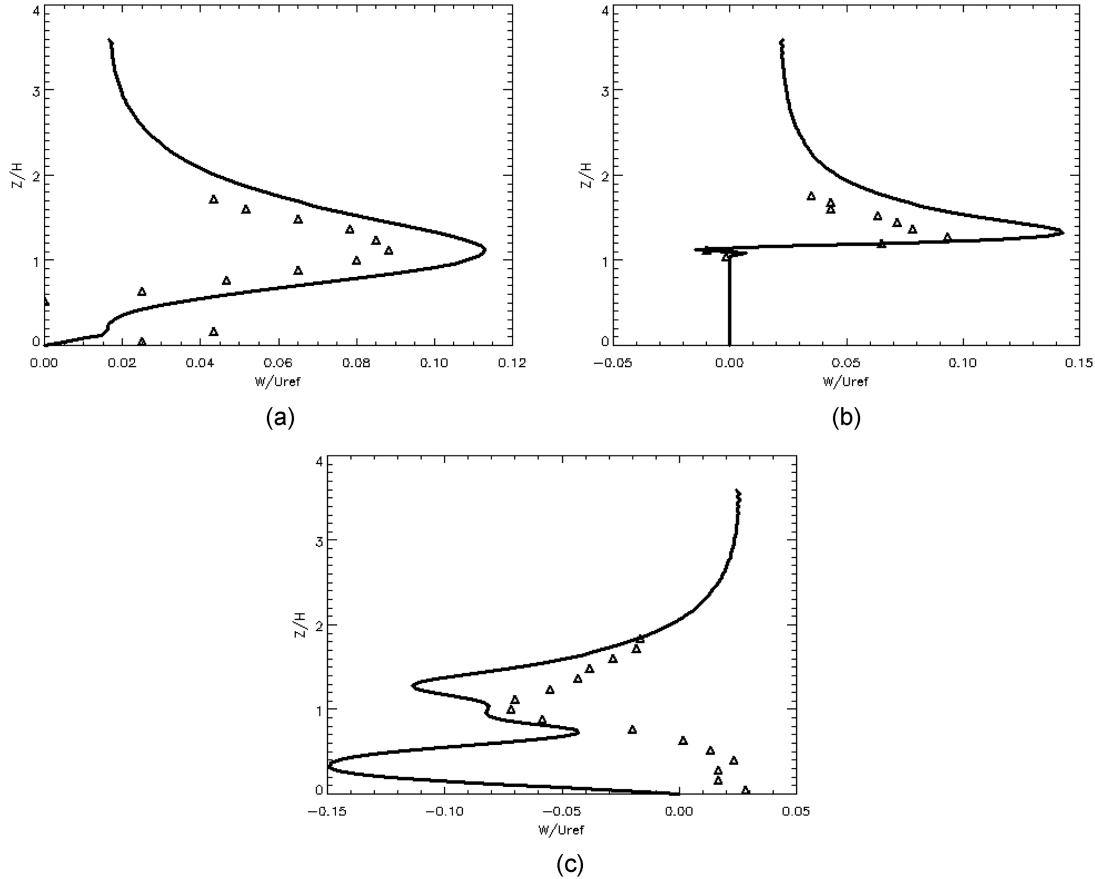


Fig. 3 The comparison of vertical profiles of w -component between CEDVAL and LES (20-min average): (a) $X/H = -0.82$; $Y/H = 0$ (b) $X/H = -0.08$; $Y/H = 0$ (c) $X/H = 1.08$; $Y/H = 0$

angle between the long axis and the surface. This is why the downwash flow in the lower part of the cavity vortex in numerical simulation result is greater than that in physical experiment result. Especially near the reattachment point, because the stronger downwash flow is blocked by the surface, the air flow has to move horizontally, the horizontal wind speed is overestimated in the lower part of the cavity vortex.

2.3. Description of simulation cases

The flow fields in a real urban neighborhood is simulated to understand the bulk impact of building on ambient wind. The distribution of buildings in simulation domain is illustrated in Fig. 4. The buildings in the central area of the domain are lower than those in the edge area. The average height of buildings is 22 m, the highest buildings are the three towers in the south of the domain, which reaches 75 m. The x coordinate in the simulation is from west to east and y is from south to north. The simulation domain is of 750 m in x direction and 540 m in y direction, the top level is 300 m. The grid resolution is 3 m and the integral time step is 0.2s. Mesh resolution plays an important role in large eddy simulation on flows features around buildings as demonstrated by Tutar and Oguz (2002,



Fig. 4 Building distribution in the simulation domain

2004). We compared the results with a resolution of 2 m and these of 3 m of case WEST (defined below). The mesh resolution impacts little on both the flow fields and the bulk average profiles, and the 3 m resolution is used in our work to save the CPU time. The whole simulation time is 30 minutes, the first 10 minutes is an adjusting period to make the buildings affect flow fully and results of later 20 minutes are analyzed to get the flow statistical characteristics.

The inflow condition is:

$$u = \cos(b) * u_0 \left(\frac{z}{z_0} \right)^a, \quad v = \sin(b) * u_0 \left(\frac{z}{z_0} \right)^a, \quad w = 0.0 \text{ m/s}, \quad u_0 = 2.0 \text{ m/s}, \quad z_0 = 10.0 \text{ m/s},$$

$$a = 0.20.$$

Z_0 is the reference height and α is wind profile exponent. Cases named WEST, NORTHWEST, SOUTHWEST are simulated standing for the inflow directions are west, northwest and southwest wind. In these cases, $b = 0$ degree in case WEST, -45 degree in case NORTHWEST and 45 degree in case SOUTHWEST respectively.

3. Results

3.1. Analysis on flow structure

The horizontal distributions of wind speed at $Z/H = 0.1$ (where H is the building height) of three cases are shown in Fig. 5 and the respective streamlines are illustrated in Fig. 6. Wind shadows appear before and behind the buildings due to the blocking of buildings. The larger the projected area of buildings on the cross wind lines, the larger the wind shadows behind them, for example, the wind shadows behind the three 'V'-shape buildings in the north of the domain are largest in NORTHWEST, moderate in WEST, and smallest in SOUTHWEST. Buildings distribution leads to a 'channeling effect' and cause a great wind speed above 3.0m/s in the area where buildings are dense. 'Channeling effect' is most apparent in WEST when the inflow is parallel with most of the buildings. Kim and Baik (2004) discussed the effect on ambient wind direction on flow and dispersion in urban street canyons and found when the incident wind

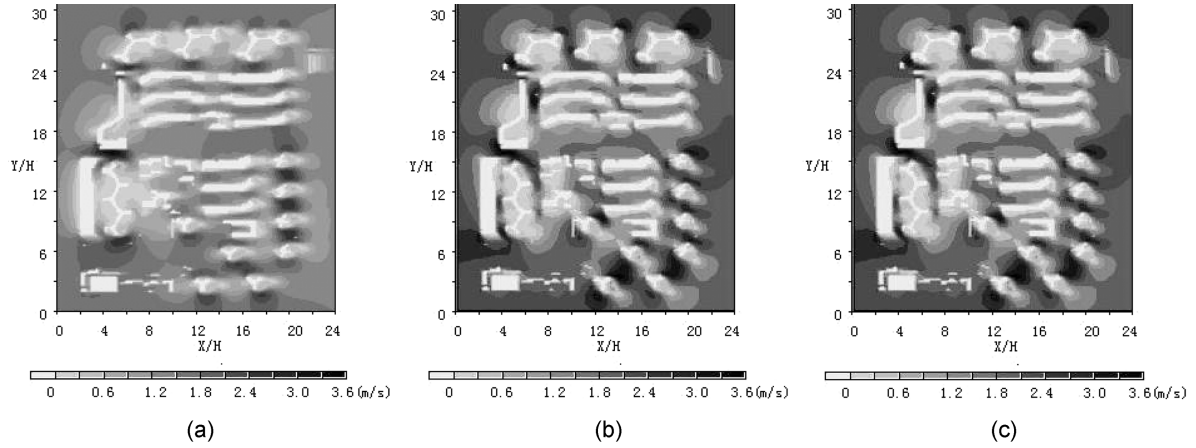


Fig. 5 The horizontal distribution of wind speed at $Z/H = 0.1$ (20-min average): (a) WEST (b) NORTHWEST (c) SOUTHWEST

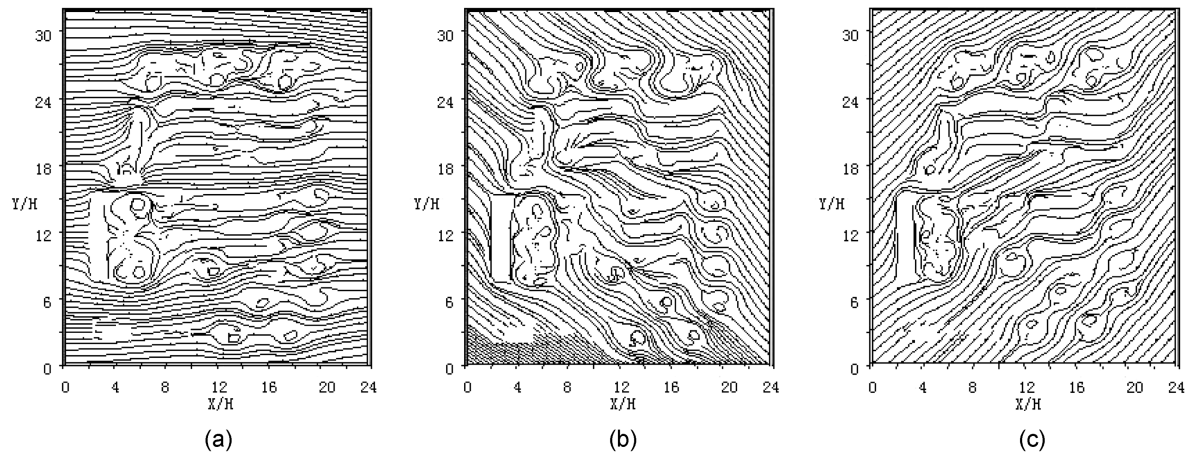


Fig. 6 Streamlines at $Z/H = 0.1$ (20-min average): (a) WEST (b) NORTHWEST (c) SOUTHWEST

angle is 45° , flow is diagonally symmetric behind the upwind building. In this paper the results show that the vortices behind the buildings are destroyed or re-shaped because of the asymmetry of building shapes and it is hard to form a double-vortex circulation there. The circulations behind buildings change greatly due to the inflow directions, especially those behind the complex irregular shape buildings.

Fig. 7 illustrates the horizontal distribution of turbulence energy at $Z/H = 0.1$. The peak value of turbulence energy appears at the upwind corners of buildings. The high value areas of turbulence energy always appear near the high, irregular-shaped buildings. Fig. 8 shows the wind speed distribution and streamlines at $Z/H = 1.6$ of the case WEST. Flows travel around buildings and form vortices behind them while in the center of the area flows are regular without the blocking of buildings. ‘Funneling effect’ is apparent at this level and wind is weakening in the center due to the drag of buildings.

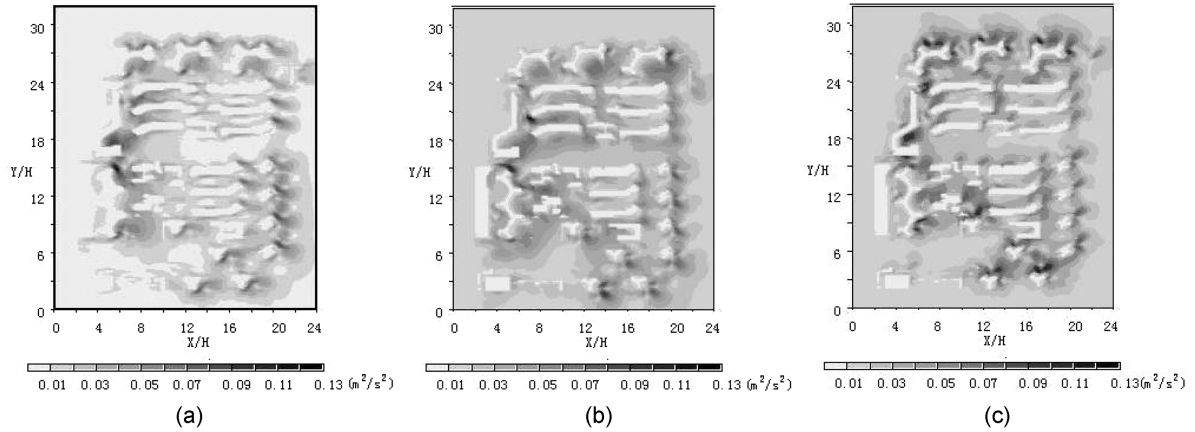


Fig. 7 Horizontal distributions of turbulence energy at $Z/H=0.1$ (20-min average): (a) WEST (b) NORTHWEST (c) SOUTHWEST

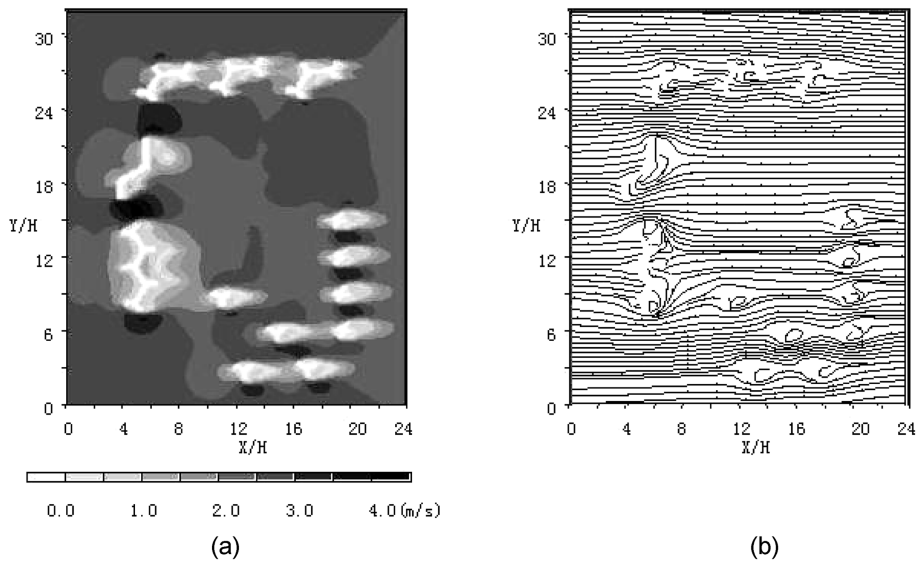


Fig. 8 Horizontal distribution of wind speed and streamlines in WEST (20-min average): (a) wind speed (b) streamlines

Fig. 9 illustrates the wind field at $Z/H = 3.5$ in WEST. The streamlines are regular because there is blocking or drag of buildings at this level. In the west and south of the simulation domain there are ‘roof jets’ above the roofs of building, where wind speed is larger than that in surrounding area. The turbulence energy distribution is similar to the distribution of wind speed; the larger wind speed area is also the larger turbulence energy area.

3.2. Bulk effect of buildings on flow

Fig. 10 shows the averaged wind profile above the buildings in three cases and the initial inflow.

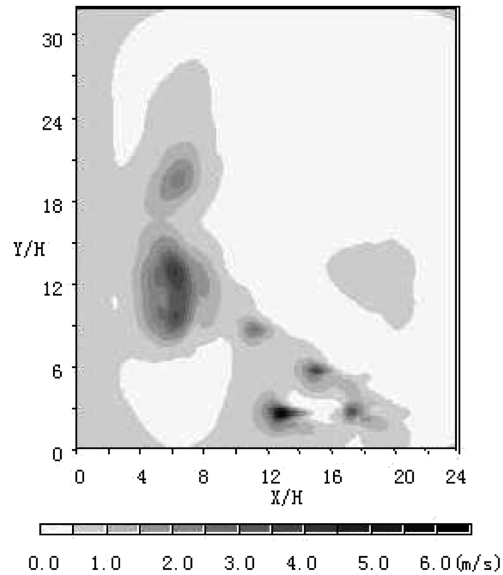
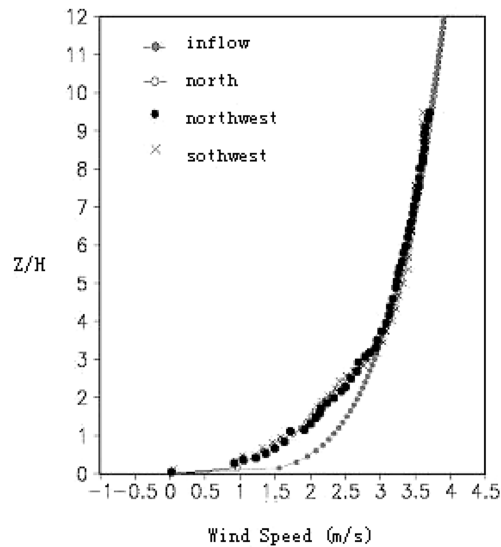
Fig. 9 Wind speed distribution at $Z/H = 3.5$ in WEST

Fig. 10 Averaged wind profiles of three cases and inflow

The wind speed at low layer is weakened due to the buildings, the height of wind weakness layer reaches about $4H$, and the height of wind speed loss peak is at $Z/H = 0.9$, a little lower than the average building height. The wind speed profiles are even the same in the three cases, while the total cross-wind area of the buildings changes greatly in the three cases. The bulk weakness due to buildings relates to the total volume or building surface area greater than to the cross-wind area. This should be noticed when parameterizing the buildings' effect in meso-scale models and more advanced research should be carried out.

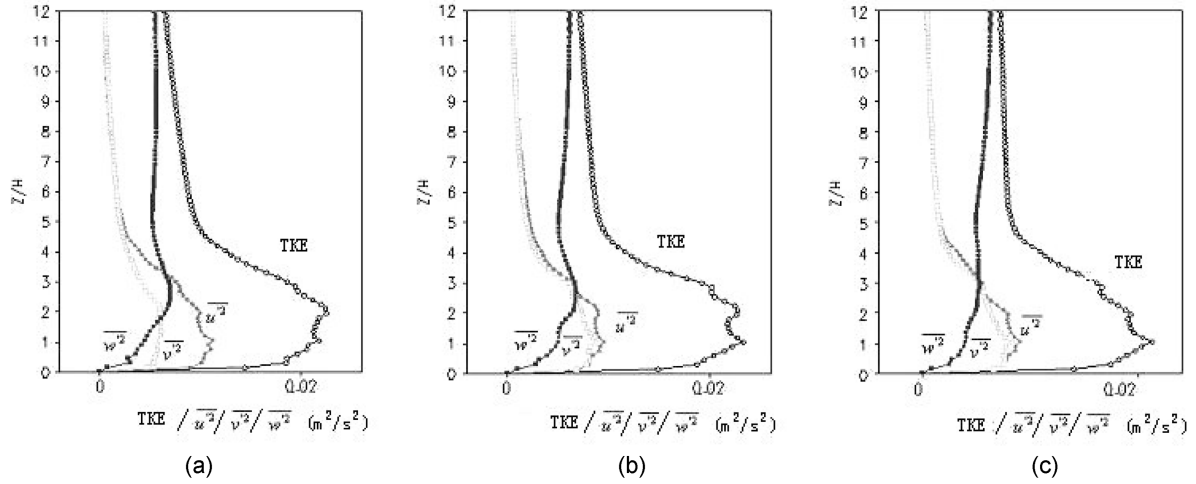


Fig. 11 The profiles of averaged turbulence energy and $\overline{u'^2}$, $\overline{v'^2}$, $\overline{w'^2}$: (a) WEST (b) NORTHWEST (c) SOUTHWEST

Fig. 11 shows the vertical profiles of averaged turbulence energy and $\overline{u'^2}$, $\overline{v'^2}$, $\overline{w'^2}$. The peak of turbulence energy appears at $Z/H = 1.0$ in all the three cases. The turbulence energy decreases with height above $Z/H = 1.0$ in the case WEST, while another peak will appear at $Z/H = 2.5$ in case NORTHWEST and case SOUTHWEST. In WEST, the $\overline{u'^2}$ contribute most of turbulence energy in low layer, and the contributions of $\overline{v'^2}$ and $\overline{w'^2}$ are less, with the height increasing, the contributions from $\overline{u'^2}$ and $\overline{v'^2}$ become less and that from $\overline{w'^2}$ increases. In NORTHWEST and SOUTHWEST, $\overline{u'^2}$ and $\overline{v'^2}$ offer most part of the turbulence energy in low layer while $\overline{w'^2}$ does little, and $\overline{w'^2}$ becomes the main source of turbulence energy in higher layer. This is mainly because that most of the buildings complexes in the simulation domain are parallel with x-axis, stronger ‘funneling effect’ appears in case WEST, which will cause greater horizontal wind speed gradient and causes stronger turbulence in horizontal directions. It is obvious in these simulations that the inflow direction affects the vertical distribution of turbulence energy little while impacts the turbulence energy partition greatly. The turbulence energy in low layer (about under $Z/H = 3.0$) comes from the fluctuation of horizontal wind components and that in high layer from the fluctuation of vertical wind component.

4. Conclusions

A large eddy simulation model is used to simulate the flows affected by a real building group to understand the detail and bulk effect of buildings on surrounding wind field. The results show:

- Wind shadows are formed before and behind buildings due to the blocking of them, wind speed is weakened because of the friction and dragging of buildings. ‘Corner jet’ and ‘roof jet’ appear at the upwind corner or above the roof of building, where always a high turbulence energy area appears.
- Inflow directions affect the flow characteristics among buildings greatly, especially the vortex structures, due to the change of cross-wind area. The effects include: the re-shaping or disappear of the wake vortices, the location and intensity of channeling effect, the area, location and intensity of wind shadows.

- (c) The buildings weaken the wind speed much in the bulk averaged wind profiles. The weakness can reach the height of four times of the average building height, the peak value of wind loss appears at $Z/H = 0.9$. The bulk averaged wind profiles change little under different inflow directions.
- (d) A peak value of turbulence energy appears at $Z/H = 1.0$ in all three cases. The turbulence energy partition changes much under different inflow directions. The contribution of the fluctuations of different wind components changes greatly with height, in low layer ($Z/H < 3.0$) the contributions from fluctuations of horizontal wind components are dominant and that from vertical wind component is dominant in the higher layer.

Acknowledgements

Sponsored by National Natural Science Foundation of China (40333027) and LAPC Open Fund Project (LAPC-KF-2004-07)

References

- Ashie, Y., Ca, W.T. and Asaeda, T. (1990), "Building canopy model for the analysis of urban climate", *J. Wind Eng. Aerodyn.*, **81**, 237-248.
- Baik, J.J. and Kim, J.J. (1999), "A numerical study of flow and pollutant dispersion characteristics in urban street canyons", *J. Applied Meteorology*, **38**, 1576-1589.
- Baskaran, A. and Kashef, A. (1996) "Investigation of air flow around buildings using computational fluid dynamics techniques", *Eng. Struct.*, **18**(11), 1-38.
- Deardorff, J. W. (1980), "Stratocumulus-capped mixed layers derived from a three-dimensional model", *Boundary Layer Meteorology*, **18**, 495-527.
- Gutman, D.P., Torrance, K.E. (1975), "Response of the urban boundary layer to heat island addition and surface roughness", *Boundary Layer Meteorology*, **9**, 217-233.
- He, J. and Song, C.C. (1997), "A numerical study of wind flow around the TTU building and the roof corner vortex", *J. Wind Eng. Ind. Aerodyn.*, **67-68**, 547-558.
- Hunter, L.J., Johnson, G.T. and Watson, I.D. (1992), "An investigation of three dimensional characteristics of flow regimes within the urban canyon", *Atmospheric Environment*, **20**, 425-432.
- Jiang, W. and Miao, S., *et al.* (2003), "Comparision and analysis of pollution of a city sug-domain scale model with wind tunnel experiment", *Acta Scientiae Circumstantiae*, **23**, 652-656.
- Jiang, W. and Miao, S. (2004), "Study on large eddy simulation and atmospheric boundary layer", *Progress in Natural Sci.*, **14**, 11-19.
- Kim, J.J. and Baik, J.J. (1999), "A numerical study of thermal effects on flow and pollutant dispersion in urban street canyons", *J. Applied Meteorology*, **38**, 1249-1261.
- Kim, J.J. and Baik, J.J. (2004), "A numerical study of the effects of ambient wind direction on flow and dispersion in urban stree canyons using the RNG k-epsilon turbulence model", *Atmospheric Environment*, **38**(18), 3039-3048.
- Launder, B.E. and Spalding, D.B. (1974), "The numerical computation of turbulent flows", *Computer Methods in Applied Mech. Eng.*, **3**, 269-289.
- Miao, S. and Jiang, W. (2004), "Large eddy simulation and study of the urban boundary layer", *Adv. Atmospheric Sci.*, **21**, 650-661.
- Murakami, S., and Mochida, A. (1987), "3-D numerical simulation of air flow around a cubic model by means of the $k-\epsilon$ model", *J. Wind Eng. Ind. Aerodyn.*, **25**, 291-305.
- Murakami, S., and Mochida, A. (1988), "3-D numerical simulation of air flow around a cubic model by means of large eddy simulation", *J. Wind Eng. Ind. Aerodyn.*, **31**, 283-303.
- Murakami, S. (1990), "Examing the $k-\epsilon$ model by means of a wind tunnel test and large eddy simulation of the

- turbulence structure around a cube”, *J. Wind Eng. Ind. Aerodyn.*, **35**, 87-100.
- Myrup, L.O. (1969), “A numerical model of the urban heat island”, *J. Applied Meteorology*, **8**, 908-918.
- Paterson, D.A. and Apelt, C.J. (1986), “Computation of wind flows over three dimensional buildings”, *J. Wind Eng. Ind. Aerodyn.*, **24**, 192-213.
- Paterson, D.A. and Apelt, C.J. (1989), “Simulation of wind flows over three dimensional buildings”, *Buildings Environment*, **24**, 39-50.
- Paterson, D.A. and Apelt, C.J. (1990), “Simulation of flow past a cube in a turbulent boundary layer”, *J. Wind Eng. Ind. Aerodyn.*, **35**, 149-176.
- Shah, K.B. and Ferziger, J.H. (1997), “A fluid mechanics view of wind engineering: Large eddy simulation of flow past a cubic obstacle”, *J. Wind Eng. Ind. Aerodyn.*, **67-68**, 211-224.
- Sini, J.F. Anquetin, S. and Mestayer, P.G. (1996), “Pollutant dispersion and thermal effects in urban street canyons”, *Atmospheric Environment*, **30**, 2659-2677.
- Sorbjan, Z. and Uliasz, M. (1982), “Some numerical urban boundary layer studies”, *Boundary Layer Meteorology*, **22**, 481-502.
- Summers, D.M., Hanson, T. and Wilson, C.B. (1986), “Validation of a computer simulation of wind flow over a building model”, *J. Building Environment*, **21**, 97-111.
- Tutar, M. and Oguz, G. (2002), “Large eddy simulation of wind flow around parallel buildings with varying configuration”, *Fluid Dyn. Res.*, **31**, 289-315.
- Tutar, M. and Oguz, G. (2004), “Computational modeling of wind flow around a group of buildings”, *Int. J. Comp. Fluid Dyn.*, **18(8)**, 651-670.
- Uno, I., Ueda, H. and Wakamatsu, S. (1989), “Numerical modeling of the nocturnal urban boundary layer”, *Boundary Layer Meteorology*, **49**, 77-98.
- Vukovich, F.M., *et al.* (1976), “A theoretical study of the St. Louis heat island: the wind and temperature distribution”, *J. Applied Meteorology*, **15**, 417-440.
- Vukovich, F.M., *et al.* (1978), “A theoretical study of the St. Louis heat island: some parameter variation”, *J. Applied Meteorology*, **17**, 1585-1594.
- Vukovich, F.M. *et al.* (1979), “Observations and simulations of the diurnal variation of the urban heat island circulation and associated variations of ozone distribution: A case study”, *J. Applied Meteorology*, **18**, 836-854.
- Yu, T.W. and Wagner, N.K. (1975), “Numerical study of the nocturnal urban boundary layer”, *Boundary Layer Meteorology*, **9**, 143-162.
- Zhang, N., Jiang, W. and Hu, F. (2004), “Numerical method study of how buildings affect the flow characteristics of an urban canopy”, *Wind and Struct., An Int. J.*, **7(3)**, 159-172.
- Zhang, N. (2004), “A eddy simulation on the effect of buildings on urban micro scale meteorological environment”, *Ph.D. Dissertation of Nanjing University, China*.
- Zhang, N. and Jiang, W. (2005), “A large eddy simulation on the effect of building on atmospheric pollutant dispersion”, *Chinese Atmosphere Science (Submitted)*.